Journal of Plant Physiology 167 (2010) 1613–1621

Contents lists available at ScienceDirect

Journal of Plant Physiology

journal homepage: www.elsevier.de/jplph

Ectopic expression of *TrPI*, a *Taihangia rupestris* (Rosaceae) *PI* ortholog, causes modifications of vegetative architecture in *Arabidopsis*

Shanhua Lü[a,b], Yinglun Fan[a], Like Liu[a], Shujun Liu[b], Wenhui Zhang[a], Zheng Meng[b,*]

[a] *School of agriculture, Liaocheng University, Liaocheng, 252059, China*
[b] *Laboratory of Photosynthesis and Environmental Molecular Physiology, Institute of Botany, Chinese Academy of Sciences, Xiangshan, Beijing 100093, China*

ARTICLE INFO

Article history:
Received 1 September 2009
Received in revised form 30 May 2010
Accepted 6 June 2010

Keywords:
Arabidopsis
B-function
MADS-box gene
PISTILLATA
Taihangia rupestris

SUMMARY

In eudicotyledonous model plants, the B-function genes encode a pair of partner MADS-domain proteins, APETALA3 (AP3) and PISTILLATA (PI) in *Arabidopsis* and DEFICIENS (DEF) and GLOBOSA (GLO) in *Antirrhinum*. These proteins, which must form heterodimers to function, are required to specify petal and stamen identity during flower development. Here, we report cloning and characterization of *TrPI* (*Taihangia rupestris PISTILLATA*), a *PI*/*GLO*-like gene from the core eudicot species *Taihangia rupestris* (Rosaceae). DNA gel blot analysis showed that *TrPI* is a single copy gene in the *T. rupestris* genome. Quantitative RT-PCR and *in situ* hybridization analyses revealed that *TrPI* is transcribed in both the vegetative and reproductive organs at different levels. Ectopic expression of *TrPI* in *Arabidopsis* caused severe modifications in vegetative plant architecture, including rosette leaves and cauline leaves arranged in a non-spiral phyllotaxy, and a flattened primary inflorescence stem that produced two or three offshoots at the base, middle or top. Moreover, we show that the *TrPI* gene is capable of rescuing *pi-1* mutant phenotypes. Yeast two-hybrid assays showed that *TrPI* forms homodimers. Taken together, these results show that *TrPI* might function in regulating plant architecture in addition to its function as a floral organ identity gene in *T. rupestris*, suggesting that the TrPI protein has biochemical features that distinguish it from the well-studied orthologs, PI and GLO.

1. Introduction

The MADS-box gene family encoding transcription factors has been subjected to extensive gene duplication events and subsequent functional divergence during plant evolution (Theissen et al., 2000; Becker and Theissen, 2003; Irish and Litt, 2005). These transcription factors control diverse developmental processes, such as regulation of flowering time, flower meristem and organ identity, fruit ripening and dehiscence, fertility, leaf development, and root architecture (Alvarez-Buylla et al., 2000; Theissen et al., 2000; Causier et al., 2002).

A large number of MADS-box genes have been isolated from angiosperms to date. These represent 13 different gene groups, namely, the *APETALA3*- (*AP3*-)/*DEFICIENS*- (*DEF*-), *PISTILLATA*- (*PI*-)/*GLOBOSA*- (*GLO*-), *AGAMOUS*- (*AG*-), *AGL6*-, *AGL12*-, *GGM13*- (*Bsister*), *TM3*-, *STMADS11*-, *AGL2*-, *AGL17*-, *APETALA1* (*AP1*)/*SQUA*-, *AGL15*- and *FLC*-like genes (Becker and Theissen, 2003). In *Arabidopsis thaliana* and *Antirrhinum majus*, the *AP3*/*DEF*-like genes (*AP3* and *DEF*, respectively) and the *PI*/*GLO*-like genes (*PI* and *GLO*, respectively) (Goto and Meyerowitz, 1994; Yang et al., 2003), encode the B-function proteins of the classic ABC model of flower development (Coen and Meyerowitz, 1991). B-function combines with A-function to specify the development of petals, and with C-function to determine the development of stamens. Mutations in either of the B-function genes result in homeotic transformations of petals into sepals and stamens into carpels. Therefore, *AP3* and *PI* in *Arabidopsis*, and *DEF* and *GLO* in *Antirrhinum* are obligate heterodimers required to specify petal and stamen identities (Sommer et al., 1990; Jack et al., 1992; Trobner et al., 1992; Goto and Meyerowitz, 1994; Jack et al., 1994). *AP3*/*DEF*- and *PI*/*GLO*-like genes appear to be highly conserved in number and function in *Arabidopsis* and *Antirrhinum*. However, in *Petunia*, another model plant in the core eudicots, two *AP3*/*DEF*-like genes, *PhDEF* (previously *Green Petals*, *GP*) and *PhTM6*, and two *PI*/*GLO*-like genes, *PhGLO1* (previously *FBP1*) and *PhGLO2* (formerly *PMADS2*) have been identified as being produced by gene duplication events (Angenent et al., 1992; Angenent et al., 1993; van der Krol et al., 1993; Tsuchimoto et al., 2000). These paralogous genes are partially redundant, but have diverged in functionality, as reflected by whorl-specific

Abbreviations: aa, amino acids; Ade, Adenine; CaMV, cauliflower mosaic virus; His, histidine; LacZ, β-Galactosidase activity; Leu, leucine; RACE, rapid amplification of cDNA ends; RT-PCR, reverse transcriptase polymerase chain reaction; Trp, Tryptophan; 3-AT, 3′-aminotriazole.

* Corresponding author. Laboratory of Photosynthesis and Environmental Molecular Physiology, Institute of Botany, Chinese Academy of Sciences, Xiangshan, Beijing, 100093, China. Tel.: +86 10 62836556; fax: +86 10 82599701.
E-mail address: zhmeng@ibcas.ac.cn (Z. Meng).

0176-1617/$ – see front matter © 2010 Elsevier GmbH. All rights reserved.
doi:10.1016/j.jplph.2010.06.028

functions and partner specificity. Thus far, numerous B class genes have been isolated and characterized from other core eudicots, basal eudicots and basal angiosperms. They show expression patterns ranging from vegetative tissues (e.g. leaves, stems, root nodules, young seedlings) to floral organs and fruits (e.g. sepals, petals, stamens, carpels, ovules) (Zahn et al., 2005). However, there are no genetic data demonstrating that potential B class genes are involved in regulating vegetative development. To date, data about MADS-box genes in the plant family Rosaceae, including plants of significant horticultural and agronomic importance, such as roses, apples, pears, peaches, apricots, almonds, plums, strawberries and many more, are scarce (Yao et al., 1999; Kitahara et al., 2001; Linden, 2002; van der Linden et al., 2002; Tani et al., 2009).

To parse the extent to which MADS-box gene functions have diversified in angiosperms, we present here a characterization of the *PI*/*GLO*-like MADS-box gene, *TrPI*, from *Taihangia rupestris* (*T. rupestris*). *T. rupestris* represents a clade that is evolutionarily distant from the Asterids *Antirrhinum* and *Petunia*, and more closely related to the Rosid *Arabidopsis* (Soltis et al., 1999; APGII., 2003). *T. rupestris* is a rosette perennial polycarpic herb species endemic to China. It belongs to the Dryadeae, Rosoideae, Rosaceae. Within the Dryadeae tribe, *T. rupestris* is a distinctive species because it is diploid, whereas other genera, such as *Dryas*, *Geum*, *Coluria* and *Waldsteinia* are polyploids. Leaf primordia are initiated from the flanks of the shoot apical meristem. The rosette leaves are arranged in a spiral phyllotaxy around the very short stem. Its flowers have both advanced and primitive features. Five sepals and petals arranged in actinomorphic morphology, numerous and apostemonous androecia and gynoecia, stamen filaments with same length, and marginal placentation represent primitive characters, whereas sepals and petals arranged alternately, partial synsepaly at the base, carpels with differentiated ovary, stigma and style are advanced. Its inflorescence stems are round. The determinate inflorescences are unusually composed of two or three florets born in the axils of each leaf (Lü et al., 2007; Du et al., 2008). Expression analyses indicate that *TrPI* is transcribed in both leaves and floral organs. Ectopic expression of *TrPI* in *Arabidopsis* causes modifications in plant architecture. The *TrPI* gene, driven under control of a double Cauliflower Mosaic Virus (CaMV) 35S promoter, can complement the floral defects of *pi-1* mutants. Yeast two-hybrid assays show that the interaction pattern of TrPI is distinct from those of PI in *Arabidopsis* and GLO in *Antirrhinum*. Based on these results, we hypothesized that *TrPI* might function in regulating plant architecture in addition to its putative function as a floral organ identity gene in *T. rupestris*.

2. Materials and Methods

2.1. Plant material

T. rupestris plants were cultivated in growth chambers under the temperature condition of 10-12 °C. Inflorescence stems, floral buds across different developmental stages, and leaves were harvested and frozen in liquid nitrogen for DNA extraction and RNA isolation, or fixed and embedded in paraplast for *in situ* hybridization

2.2. Cloning of TrPI

Total RNA was isolated using Plant RNA Purity Reagent (Invitrogen) from the inflorescences of *T. rupestris* at the floret differentiation stages. Poly (A)$^{\pm}$ mRNA was purified from total RNA using the Oligotex mRNA Mini Kit (Qiagen). First strand cDNA was synthesized by SuperScript^{TM} III Reverse Transcriptase (Invitrogen) with a polyT primer PTA with a 5′ adapter sequence. Hemi-nested PCR amplification was performed with the degenerate MADS-box sequence forward primer B2 and the adapter primer AP. The amplified fragments of about 1.0 kb (kilobase pair) were cloned into the pGEM-T vector (Promega) and sequenced. To obtain the 5′ partial cDNA ends of *TrPI*, 5′ rapid amplification of cDNA ends (5′ RACE) was used. Internal gene-specific primers P3PI1, P3PI2 and P3PI3 were designed for *TrPI*. The full-length cDNA of *TrPI* was obtained by 3′ RACE with primers 3N72 and AP. Sequencing of cDNAs was performed with the ABI PRISM dye terminator kit (PE Applied Biosystems, Foster City, CA). The final sequence has been deposited in GenBank under accession number DQ248947. All the primer sequences discussed in this study are shown in Table S1.

2.3. Genomic DNA extraction and DNA gel blot analysis

Genomic DNA was extracted and DNA gel blot hybridization was performed as published previously (Lü et al., 2007). A 3′ end fragment lacking of the MADS domain and partial I domain of *TrPI* (nucleotides 211-839 counted from the start codon ATG) was labeled with [$^{a\text{-}32}$P] dCTP using Prime-a-Gene® label as a probe.

2.4. Sequence analysis of TrPI and construction of phylogenetic tree

Protein sequences were aligned using CLUSTALW1.81 under default settings and refined by hand. We generated neighbor-joining (NJ) trees based on the aligned full-length protein sequences comprising the MADS, I, K, and C domains using the MEGA4 (Molecular Evolutionary Genetic Analyses, version1.1, Pennsylvania State University) package. Bootstrap values were based on 1,000 replicates. Gaps were encoded as missing data.

2.5. Vectors construction and Arabidopsis transformation

The full-length *TrPI* cDNAs were amplified using Ex-Taq DNA polymerase (TaKaRa) with a forward primer TrPIBam and a reverse primer TrPISal harboring *Bam*HI and *Sal*I site, respectively. The PCR products were cloned between the *Bam*HI and *Sal*I restriction site into pFP101 vector, which placed *TrPI* transcription under the control of a $2 \times 35S$ promoter in the sense orientation. The 35S::*TrPI* construct described above was introduced into wild-type Columbia and heterozygous *PI*/*pi-1 A. thaliana* plants by the floral dip method (Clough and Bent, 1998). The Homozygous *pi-1* plants were identified and the transgenic plants were analyzed as published previously (Lamb and Irish, 2003; Su et al., 2008).

2.6. RNA in situ hybridization and RNA gel blot hybridization

In situ hybridization and RNA gel blot hybridization methods used here have been reported previously (Li et al., 2005; Lü et al., 2007). The less-conserved sequences (nucleotides 568-899 counted from the start codon ATG) were used as the template to synthesize the probes for the *in situ* hybridization and RNA gel blot analyses.

2.7. Yeast two-hybrid assays

The two-hybrid system, *Saccharomyces cerevisiae* strain, activation domain (AD) cloning vector, and DNA-binding domain (DNA-BD) cloning vector used here, as well as the methods of constructing the fusion protein vectors, yeast transformation and interactions analysis were performed as described previously (Lü et al., 2007). Yeast two-hybrid assays were performed using the GAL4-based MATCHMAKER Two-Hybrid System (Clontech). *Saccharomyces cerevisiae* strain AH109, GAL4 activation domain (AD) cloning vector pACT2 and GAL4 DNA-binding domain (DNA-BD) cloning vector pAS2 were used. Full-length cDNA of *TrFUL*, *TrAP1*,

TrPI, *TrAG*, *TrSHP* and *TrSEP3* were amplified by PCR with *Nco*I restriction enzymes digest site at the 5′ end at the start codon and *Bam*HI at the 3′ end, as well as *Nco*I and *Eco*RI sites were introduced for *TrTM6*, and then digested using restriction enzymes for cloning into pACT2 and pAS2, respectively. All constructs were verified by sequencing. Yeast transformation was performed using the lithium acetate method. The transformants co-transformed with BD and AD fusion plasmids were confirmed by growth on dropout medium lacking leucine (Leu) and Tryptophan (Trp) and by PCR and restriction enzymes analyses. Interactions were analyzed on the selective dropout medium lacking Leu, Trp, Adenine (Ade) and histidine (His) supplemented with 20 mM 3′-aminotriazole (3-AT), and by β-Galactosidase activity (LacZ) assay. Growth of yeast on selective media was scored after 3 d of incubation at 30 °C. The LacZ activity was measured by the colony-lift filter assay and the colonies that turned blue in less than 7 h were selected. All assays were performed according to the manufacturer's protocols. Two independent transformations for each vector combination were performed and four colonies per transformation were used for the assay. The transformants co-transformed with plasmids encoding AP3 and PI from *A. thaliana* lacking MADS domains were used as a positive control, and the transformants containing plasmids pACT2 (empty construct) and pAS2 (empty construct), where no any foreign DNA or cDNA fragments were inserted were used as a negative control.

2.8. Microscopic analysis

Materials were immediately fixed in FAA (5: 6: 89 formalin: acetic acid: 50% ethanol) solution. For light microscopy, the primary inflorescence stems of transgenic plants and those of wild-type plants were embedded in Paraplast, sectioned, and then stained with 10% potassium periodate solution for 10 min, rinsed in distilled water for 1 min, Schiff's reagent for 1 min, 10% potassium pyrosulfite solution for 2 min (for three times), rinsed in distilled water for 1 min, and followed by hematoxylin for 10 min. The samples were observed with a Leica microscope (DMRB, Northvale, NJ, USA) with a digital camera (Harvard Imaging Facility). For scanning electron micrograph (SEM) analysis, the materials were treated, dried in liquid CO_2, coated with gold and observed as published previously (Xu et al., 2005). SEM was performed on a Hitachi S-800 scanning electron microscope.

2.9. Semiquantitative reverse transcriptase polymerase chain reaction (RT-PCR) and quantitative real-time RT-PCR analysis

For semiquantitative RT-PCR and quantitative real-time RT-PCR analysis on *TrPI* transcripts in various *T. rupestris* tissues, the extraction of total RNA, purification of mRNA, and synthesis of first strand cDNA were carried out according to the methods as described in the cloning of *TrPI*. For semiquantitative RT-PCR reaction, the *TrPI* locus-specific forward primer TrPIF1 and reverse primer TrPIR1 were designed and used to amplify cDNA from different tissues to detect *TrPI* expression profiles. Primers to actin were used as a positive control. The *T. rupestris actin*-specific forward primer TrACF and reverse primer TrACR1 were designed according to the *T. rupestris actin* gene sequence (Du et al., 2008). The semiquantitative RT-PCR reaction conditions: 35 cycles of 30 s at 95 °C, 45 s at 58 °C, 1 min at 72 °C, preceded by 2 min at 94 °C, and followed by 10 min at 72 °C. The semiquantitative RT-PCR experiment was repeated three times to confirm the results. The identity of the amplified fragments was confirmed based on amplification product size and restriction pattern using *Sph*I.

Real-time RT-PCR was performed using the Brilliant_SYBR Green QPCR Master Reagent Kit (Stratagene, La Jolla, CA, USA) and a Stratagene Mx3000P detection system (Stratagene, La Jolla, CA, USA) as described in the manufacturer's manual. All experiments were performed with three replicates. Reaction specificities were tested with melted gradient dissociation curves, electrophoresis gels, and sequencing of each PCR product. Specific primer pairs were designed using Primer Express 3.0 software (Applied Biosystems, Foster City, Calif). The amplification of the *ACTIN* gene was used for normalization. For real-time RT-PCR analysis on *TrPI* transgene expression levels in the *Arabidopsis* plants, the extraction of total RNA, synthesis of the first strand cDNA and the PCR conditions were done according to Su et al (2008). The gene-specific forward and reverse primers used were as follows: TrPIF2 and TrPIR2 (for *TrPI*); TrACF and TrACR2 (for *T. rupestris actin*); AtPIF and AtPIR (for *Arabidopsis AtPI*); AtACF and AtACR (for *Arabidopsis actin*, At3g18780). A negative control with the cDNA template replaced by water was included in the same PCR run for each primer pair.

3. Results

3.1. Isolation and sequence analyses of TrPI from T. rupestris

A cDNA of a MADS-box gene was cloned from *T. rupestris*. A BLAST search in GenBank and sequence analyses revealed that the gene exhibits high sequence similarity to *PI*/*GLO*- like genes. Therefore, the gene is named *TrPI* (*Taihangia rupestris PISTILLATA*). Conceptual translation of the cDNA reveals that the TrPI protein has 209 amino acids (aa). TrPI has a 59-aa MADS domain, 28-aa I domain, 62-aa K domain and 60-aa C domain (Fig. 1A). Alignment of the predicted amino acid sequence of TrPI with those of PI/GLO-like proteins from *Arabidopsis*, *Antirrhinum*, *Petunia* and from Rosaceae species indicated that they share high similarities throughout the M (89.4-94.2%), I (62.5-85.1%) and K (80.7-93.3%) domains (Fig. 1A; Table S2). At the full-length protein level, however, TrPI is 48.2%, 53.2%, 55.4%, 56.8% identical to PI in *Arabidopsis*, GLO in *Antirrhinum*, and phGLO1 and phGLO2 in *Petunia*, respectively. Three regions of the heptad $(abcdefg)_n$ repeats previously identified in the K-domain, namely K1 (87-108), K2 (121-135), and K3 (143-168) subdomains (Yang et al., 2003), were also found in the TrPI protein. TrPI possesses highly conserved K1 and K2 subdomains. However, K3 is relatively less well conserved and not always occupied by hydrophobic amino acids at position **a** and **d**, like the case observed in other MADS-domain proteins (Yang et al., 2003). A highly conserved sequence KHExL also was observed at position 82-86 of TrPI, as identified in *PI*/*GLO*-like homologs (Kramer et al., 1998). Between K1 and K2, the typical sequence characteristics of almost all MIKC MADS-domain proteins were also found in the TrPI, e.g. glycine at position 110 and the hydrophobic residues at positions 113 and 116. Furthermore, several characteristic positions were also identified, e.g. position 97 negatively charged, Asn-98 in K1 specific for the DEF/GLO proteins, Gly-131 in K2 diagnostic for the PI/GLO-like proteins (Fig. 1A) (Theissen et al., 2000; Yang et al., 2003). In the C-terminal domain, the highly conserved PI motif was also observed, although the domain is less well conserved (Fig. 1A) (Kramer et al., 1998). In all phylogenetic trees (neighbor joining, maximum likelihood, and maximum parsimony trees), the hypothesis that *TrPI* belongs to the *PI*/*GLO* lineage was well supported. The support value for the *PI*/*GLO* clade was very high (96-100%) (data not shown). Furthermore, the detailed phylogenetic analysis (Fig. 1B) showed that *TrPI* falls within a well-supported clade that includes *PI*/*GLO*-like genes isolated from some Rosaceae species and the Brassicaceae plants (*PI* from *Arabidopsis*) (Kitahara et al., 2001; Yao et al., 2001; Kitahara et al., 2004; Vandenbussche et al., 2004; Zhang et al., 2008). This is in accordance with the taxonomic position of the species involved; *T. rupestris* belongs to the Rosaceae, whereas *Petunia* and *Antirrhinum* belong to the Asteridae. Remark-

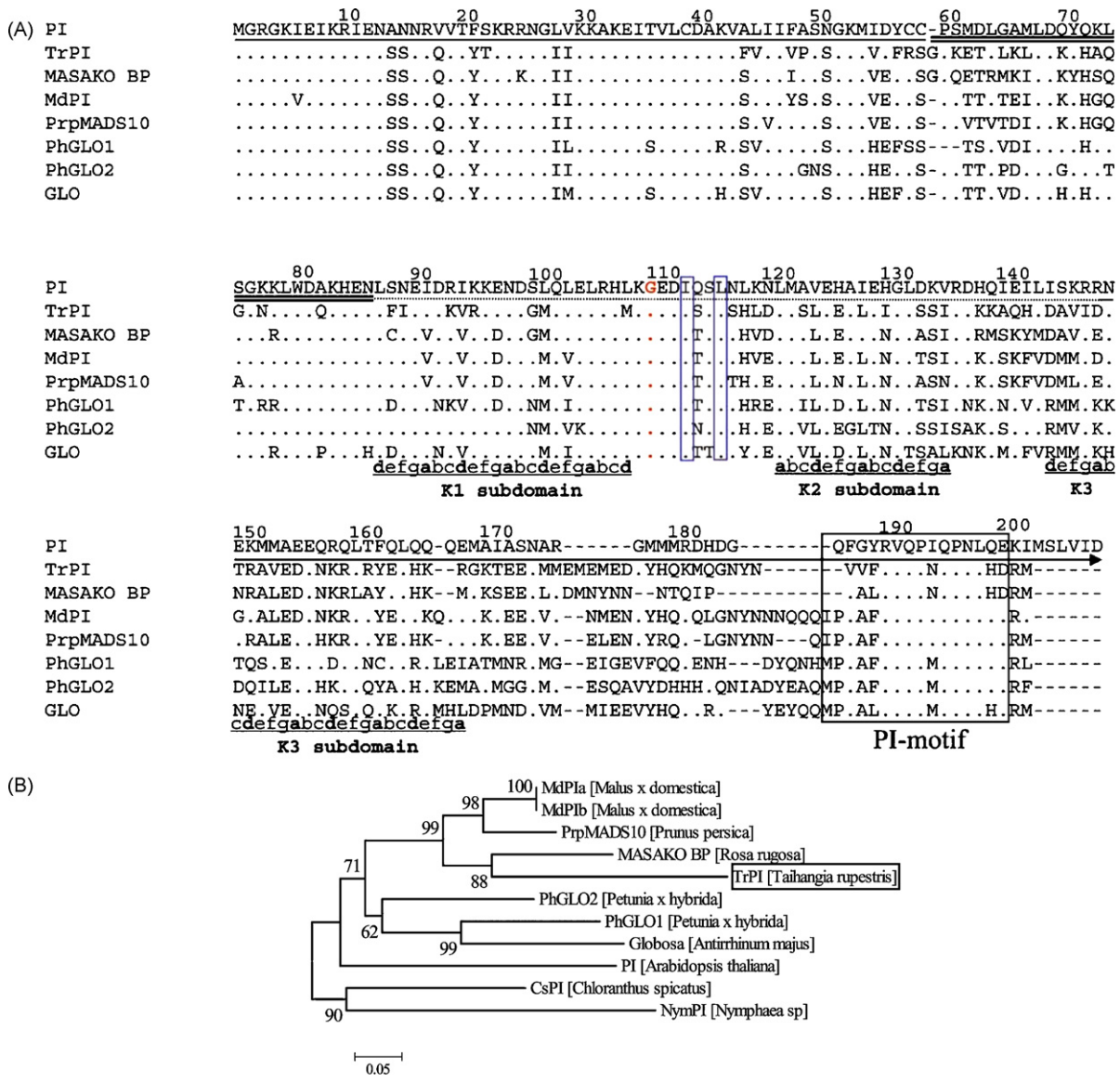

Fig. 1. A. The alignments of the predicted amino acid sequences of TrPI from *T. rupestris* with representatives of other PI-related proteins. The dots (.) indicate identical amino acid to PI and gaps (-) are introduced to maximize alignment. MADS, I, K and C domains are underlined and defined by single, double, dash line and arrow respectively, according to (Ma et al., 1991). Heptad $(abcdefg)_n$ repeats identified by Yang et al. (2003) in the K domain are represented by K1, K2 and K3 subdomains. Hydrophobic amino acids occupy the positions 113 and 116 like the same observed in most MIKC-type MADS-box proteins and are highlighted in the blue box. The highly conserved region termed PI motif is highlighted in a black box. Conserved Gly-110 is marked in red. Representatives of other MADS-box proteins: PI (AAD51988) from *Arabidopsis thaliana*, MASAKO BP (BAB11939) from *Rosa rugosa* Thunb. ex Murray, MdPI (CAC28022) from *Malus x domestica*; PrpMADS10 (ABS32248) from *Prunus persica*, PhGLO1 (AAS46018) and PhGLO2 (CAA49568) from *Petunia*. GLO (Q03378) from *Antirrhinum*.

Fig. 1. B. Phylogenic analyses of representative of *PI*-related MADS-box genes. TrPI from *T. rupestris* is boxed. The tree was rooted with NymPI from *Nymphaea sp. EMK-2003* and CsPI from *Chloranthus spicatus*. The accession numbers of the sequence data used are as follows: TrPI (ABB59993), MASAKO BP (BAB11939), MdPIa (CAC28022), PrpMADS10 (ABS32248), MdPIb (BAC11906), PhGLO1 (AAS46018), PhGLO2 (CAA49568), PI (AAD51988), NymPI (AAR87705), CsPI (AAF73939), Globosa (CAA48725). The name of the associated genus is listed in brackets after the gene name.

ably, in the phylogenetic tree, all PI/GLO-like proteins sequence isolated from the Rosaceae were included. In *Prunus* and *Rosa*, only one *PI*/*GLO*-like gene, *PrpMADS10* and *MASAKO BP*, respectively, has been identified thus far (Kitahara et al., 2001; Zhang et al., 2008). However, in the genus *Malus*, Yao et al. (2001) isolated two cDNA of *PI*/*GLO*-like genes from the cultivar "Granny Smith," and both genes were termed previously as *MdPI* (Yao et al., 2001). To facilitate description, we arbitrarily renamed the two genes *MdPIa* (accession number AJ241490) and *MdPIb* (accession number AJ241491). Only one amino acid difference was observed throughout the coding region between MdPIa and MdPIb. In addition, MdPIa and MdPIb showed 99.53% identity at the amino acid level, indicating that MdPIa and MdPIb are most likely alleles from the same locus. In another cultivar "Indo", a *PI*/*GLO*-like gene, *MdiPI*, was identified (Kitahara et al., 2004). The truncated MdiPI lacking a partial MADS domain indicated 100% identity at the amino acid levels with the corresponding part of the MdPIb, although only a partial 3′ end cDNA fragment was obtained. Therefore, there is no unequivocal evidence for gene duplications in the *PI*/*GLO*-like lineage in Rosaceae based on the current phylogenetic tree. In *T. rupestris*, *TrPI* is a single copy gene, as revealed by DNA gel blot hybridization analysis (Fig. S1). Taking these results together, we conclude that the single copy *TrPI* is the *PI* ortholog in *T. rupestris*.

3.2. Expression patterns of TrPI in T. rupestris

To determine the expression patterns of *TrPI* in *T. rupestris*, semiquantitative RT-PCR and quantitative real-time RT-PCR were

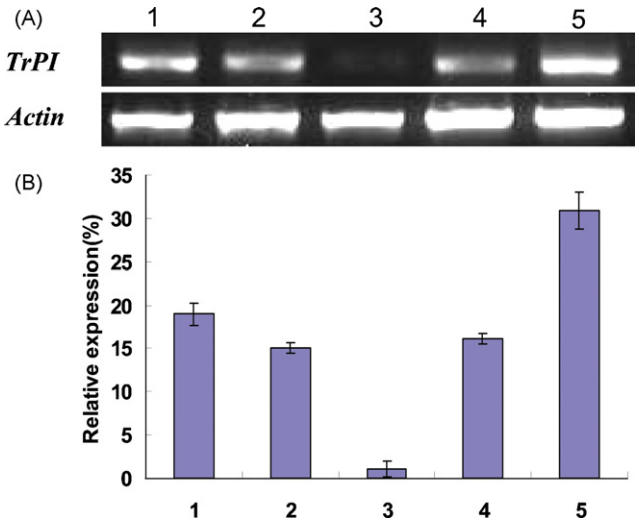

Fig. 2. Semiquantitative RT-PCR and quantitative real-time RT-PCR analysis on *TrPI* transcript levels in various *T. rupestris* tissues. 1: Leaves (<2 cm); 2: Leaves (2-4 cm); 3: Leaves (≥4 cm); 4: Infloresence Stems (<2 cm); 5: Flowers (<2 cm). A: Semiquantitative RT-PCR analysis. B: Real-time RT-PCR quantification of *TrPI*, relative to *actin*. Values are mean and standard error (error bars ± SE) of three replicates.

performed. *TrPI* was expressed in flowers, inflorescence stems and leaves, but at different levels (Fig. 2A, B). *TrPI* was more strongly expressed in flowers than in leaves and inflorescence stems (Fig. 2A, B). In leaves, *TrPI* was expressed at higher levels in young leaves than in old ones; at late stages of leaf development, the expression signals of *TrPI* were almost undetectable (Fig. 2A, B). To further investigate the spatial and temporal expression patterns of *TrPI*,

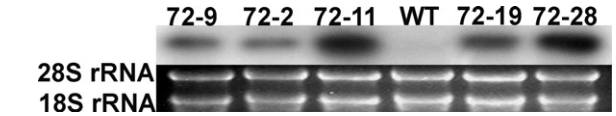

Fig. 4. RNA gel blot analyses of constitutive expression of *TrPI* in *Arabidopsis* leaves. 72-2, 72-9, 72-11, 72-19, 72-28, 35S:: *TrPI* transgenic *Arabidopsis* lines; WT, wild type *Arabidopsis* leaves.

in situ hybridization was performed at a series of developmental stages of floral buds and leaves. At early stages of floral development, *TrPI* transcripts were restricted to the meristematic domes that will give rise to the petal and stamen primordia (Fig. 3A). Subsequently, *TrPI* was expressed in the petal and stamen primordia, and in developing petals and stamens (Fig. 3B, C). At late stages of stamen and carpel development, *TrPI* expression was detected in the pollen grains, ovary, and the ovules (Fig. 3D, E). Furthermore, the accumulation of the *TrPI* mRNA was strong in the leaf primordia, but weak in developing leaves (Fig. 3F).

3.3. Ectopic expression of TrPI causes modifications in the architecture of Arabidopsis

To gain further insight into the function of *TrPI*, we overexpressed *TrPI* in wild-type *Arabidopsis* plants. Among 51 35S:: *TrPI* independent transgenic lines, 22 displayed severe phenotypes (43.1%) and 10 weak phenotypes (19.6%). Ectopic expression of *TrPI* in *Arabidopsis* was confirmed by RNA gel blot analysis from five plants that had been independently transformed with the construct (Fig. 4). Transgenic lines 72-11 and 72-28 showed higher RNA expression levels of *TrPI* together with stronger phenotypes, compared to lines 72-2, 72-9 and 72-19 with lower expression levels

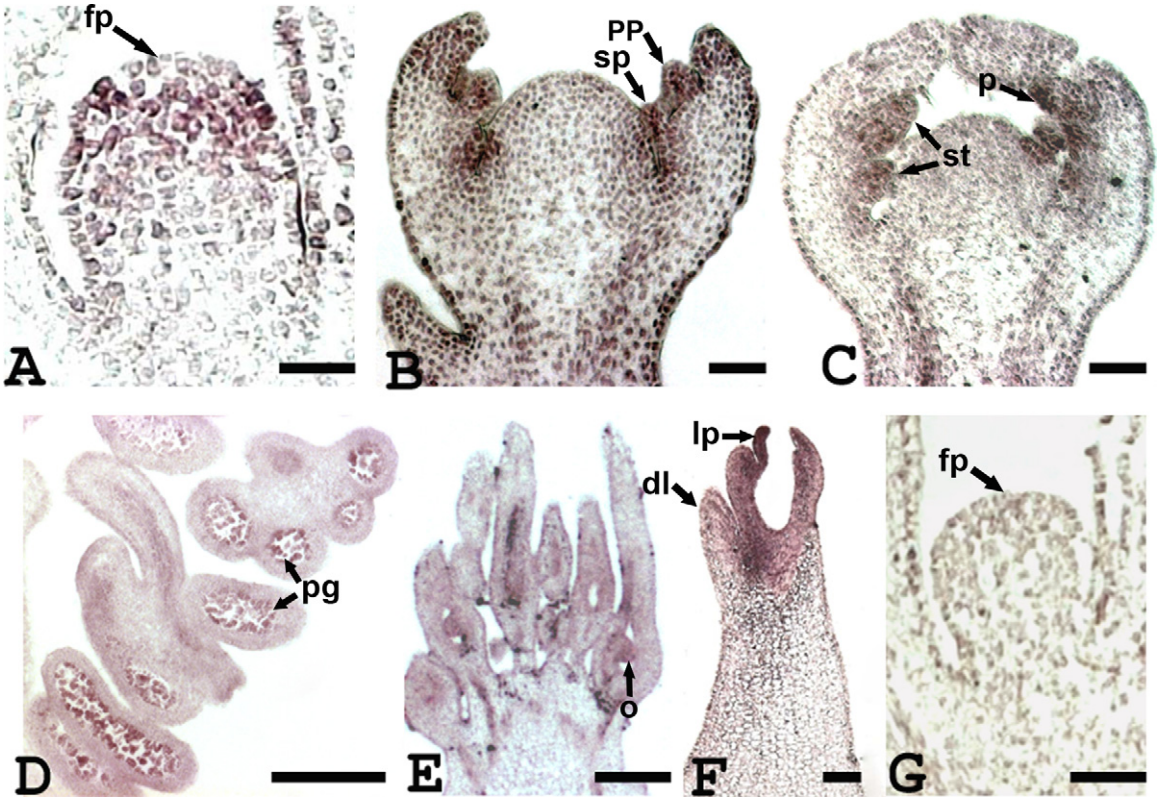

Fig. 3. *In situ* localization of *TrPI* transcripts in *T. rupestris*. **A.** The *TrPI* signal is seen in the meristematic domes that will give rise to the petal and stamen primordia. **B** and **C**. *TrPI* is expressed in the petal and stamen primordia, and in developing petals and stamens. **D** and **E**. The *TrPI* expression is detected in the pollen grains, ovary, and the ovules in the mature flower. **F.** The *TrPI* mRNA is strong in the leaf primordia, but weak in developing leaves. fp, floral primordium; pp, petal primordium; p, developing petal; sp, stamen primordium; st, developing stamen; pg, pollen grains; o, ovule; lp, leaf primordium; dl, developing leaves; Bar = 50 μm.

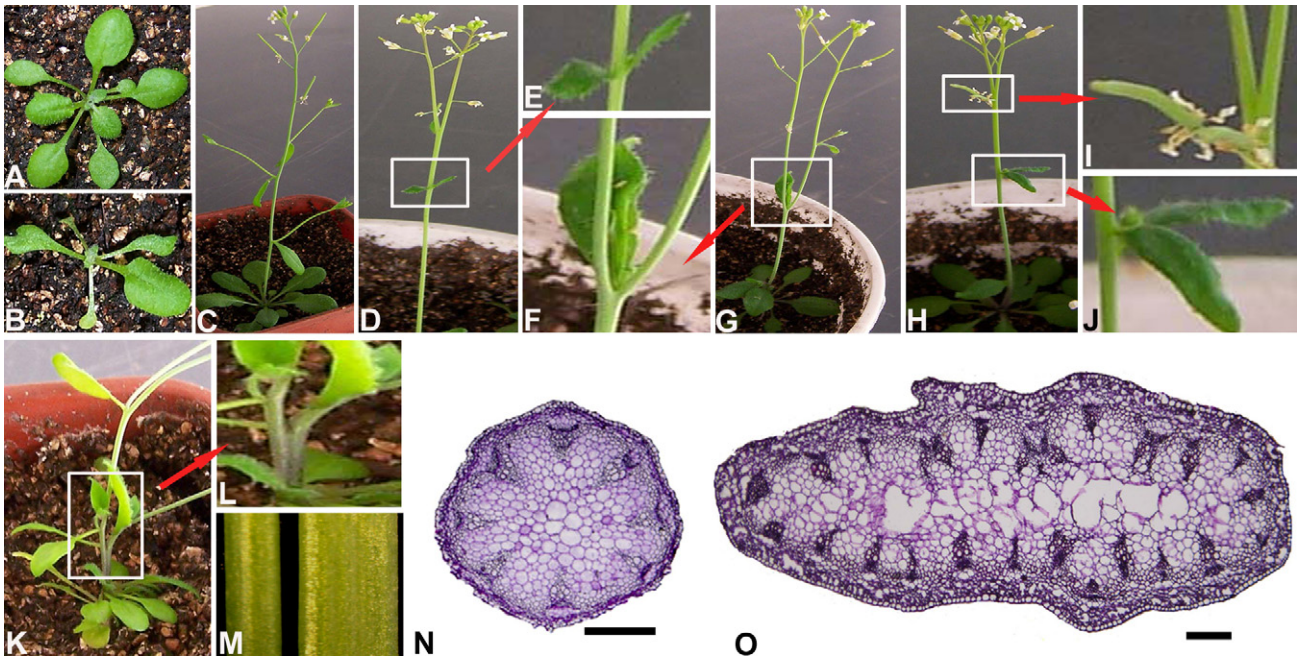

Fig. 5. *TrPI* overexpression in wild-type *Arabidopsis* plants. A, Wild type plants grown for 11d; B, 35S::*TrPI* transgenic plants grown for 11d, thin and narrow rosette leaves arranged in a non-spiral phyllotaxy in comparison with section A; C, Wild type plants grown for 27 d; D-L, 35S::*TrPI* transgenic plants grown for 27 d; N-O, Transverse sections of the primary inflorescence stem of wild type and that of 35S::*TrPI* transgenic *Arabidopsis* plant, respectively; D, Two cauline leaves emerge on opposite sides of a single node and laminaes are horizontal with dorso-ventral polarity of normal leaves; G-H, Two cauline leaves emerge side by side from a single node and laminaes are erect with abaxial surfaces pressed together (in G) or laminaes are horizontal with the dorso-ventral polarity of normal leaves (in H); G, H, K, The oblate primary inflorescence stem produced the two or three offshoots at the midst, top, or base, respectively; E, F, L, Close-up of section D, G, K, marked in the white box, respectively; I and J, Close-up of section H marked in the white box (upper and bottom, respectively). M, The primary inflorescence stem of wild type and that of 35S::*TrPI* transgene plant (left and right, respectively). Scale bar = 800 μm.

and mild phenotypes (Fig. 4). Hence, the level of transgene expression and the severity of the mutant phenotype were positively correlated. The *35S*:: *TrPI* transgenic lines 72-11 and 72-28 were selected for further analyses. The flowers of *35S*:: *TrPI* transgenic *Arabidopsis* plants showed no observable phenotype alterations. But, strikingly, architecture abnormalities were observed. The true leaves became thin and narrow (Fig. 5B). Rosette leaves were arranged irregularly and their initiation was delayed (Fig. 5B; Table S3). Numbers of the lines with aberrant rosette leaves were 32 out of 51 (62.7%) (Table S3). The rosette leaves were initiated 2.5 days later in the *TrPI* over-expressed plants than in wild-type plants (data not shown). Two cauline leaves emerged from opposite sides of a single node and were horizontal with dorso-ventral polarity of normal leaves (25.5%) (Fig. 5D, E; Table S3). Two cauline leaves emerged side by side from a single node and were erect with abaxial surfaces pressed together (17.6%) (Fig. 5F, G; Table S3) or were horizontal with the adaxial polarity of normal leaves (19.6%) (Fig. 5H, J; Table S3). The proportion of cauline leaves with aberrant arrangement was about 54.4% on average in the transgenic plant (Table S4). The primary inflorescence stem became flat (Fig. 5M) and produced two or three offshoots at the base (5.9%), middle (19.6%) or top (37.3%) (Fig. 5D, F-I, and K-L; Table S3). To observe further the cell structure of the oblate primary inflorescence stem, paraffin sections were performed. Comparison of cross-sections of the transgenic and wild-type inflorescence stems indicated that the vascular cylinders were multiple and were arranged like an oval, which is likely to result in the oblate inflorescence stem. In addition, partial pith parenchyma cells were subjected to cracking and formed a hollow in the middle of the inflorescence stem (Fig. 5O). To determine whether TrPI was able to compensate for the absence of wild-type PI protein, we overexpressed *TrPI* gene in a *pi-1* homozygous mutant background. *pi-1* is a strong allele of *PI* that contains a premature stop codon, producing a truncated protein product of 79aa. *pi-1* flowers have strong floral organ identity transformation of petals to sepals in floral whorl 2 and stamens to carpels in the whorl 3 that is fused with the central gynoecium about the position from the base to the middle (Goto and Meyerowitz, 1994). In addition, we also observed that the carpels in the positions normally occupied by the whorl 4 may not be completely fused and some ovules were exposed (Fig. 6A). In our complementation analysis, we generated transgenic lines in which the *TrPI* coding region was driven by the double 35S promoter of the Cauliflower Mosaic Virus (CaMV). Seventy-six independent transgenic lines were obtained and assayed. In addition to vegetative phenotypic alterations of 35S:: *TrPI pi-1* transgenic plants mimicking those of ectopic expression of *TrPI* in wild-type *Arabidopsis*, the *TrPI* gene can largely rescue the *pi-1* mutant phenotypes. These transformants showed a range of phenotypes (Fig. 6). To facilitate description, 'no rescue', 'weak rescue', 'strong rescue' and 'full rescue' were defined according to the degree of rescue of the *pi-1* mutant phenotype. *pi-1* mutant and wild-type flowers are shown for comparison (Fig. 6A and G). Flowers of no rescued plants were indistinguishable from *pi-1* mutant flowers (data not shown). In weak rescue lines, both the petals and stamens were not completely rescued. Filament-like structures formed in stamen positions (Fig. 6B -C). The epidermal petal cells of weak rescued plants (Fig. 6I) were more similar to those of the wild-type sepals (Fig. 6M). In flowers of strongly rescued plants, petals were slightly green, but smaller than those of wild-type petals (Fig. 6D); the stamens were also often short with occasional papillae characteristic of carpels on tips and did not shed pollen (data not shown). SEM analysis showed that the epidermal cells of the rescued petals (Fig. 6J) were more similar to those of wild-type petals (Fig. 6L), but contained stomata (Fig. 6J, arrow), which are found in wild-type sepals but not petals (Fig. 6L-M). In flowers of fully rescued plants, the petals were white, but narrow and short; the stamens were short and not fully extended,

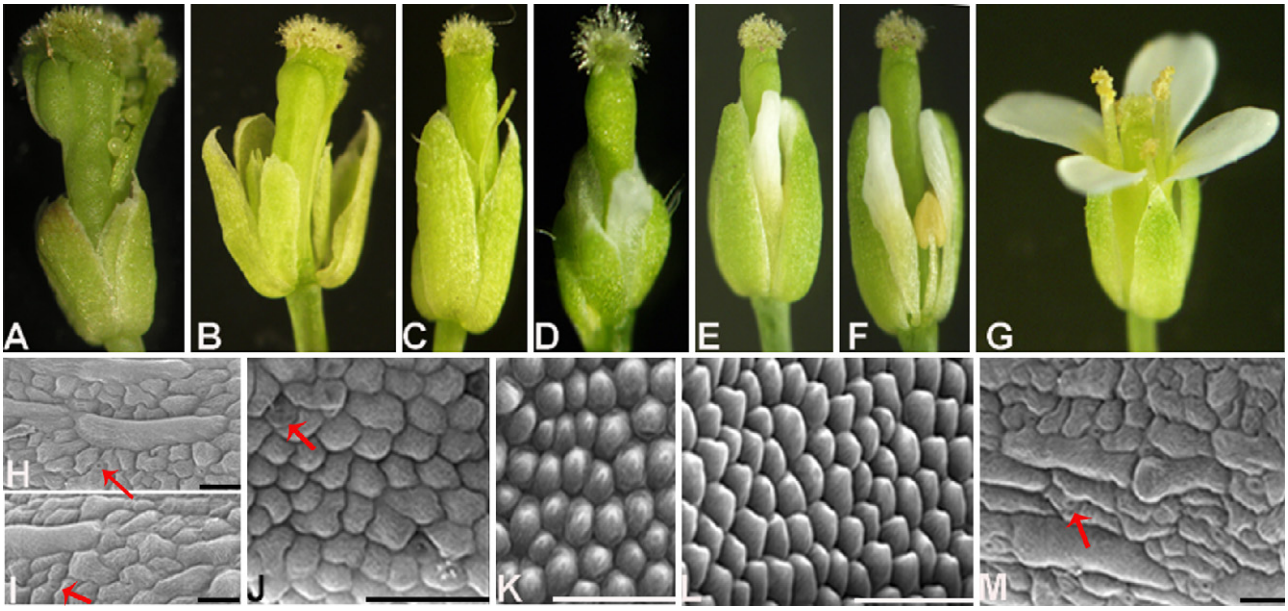

Fig. 6. Complementation analysis of *Arabidopsis pi-1* mutant by *TrPI*. A, *pi-1* mutant flower. Petals are transformed into sepal-like structures in the floral whorl 2 and stamens to carpels in the whorl 3 that is fused with the central gynoecium about the position from the base to the midst, the carpels in the whorl 4 cannot fuse well and some ovules are exposed; B-F, Flowers from different 35S:: *TrPI pi-1* lines showing different degrees of phenotypic rescue; B, Weak rescue, greenish sepaloid petals; one sepal was removed; C, Weak rescue, filament-like stamens; D, Strong rescue, slightly green petals but short; E and F, Fully rescue; white but narrow and short petals; short stamens but pollen grains produced; one sepal was removed in F; G, Wild-type flower; H-M, SEM micrographs of the epidermal cells of the sepals or petals; H, Petal epidermis of *pi-1* mutant flower; I, J and K, Petal epidermis of the flower shown in B, D and F, respectively; L and M, Petal and sepal epidermal cells of wild-type flower, respectively. Stomata are highlighted using red arrow. Scale bar = 25 μm.

but could produce fertile pollen grains (Fig. 6E-F). Moreover, the epidermal cells of rescued petals in these plants were characteristically rounded (Fig. 6K), resembling those of the wild type (Fig. 6L). Among 76 independent transgenic lines, 2 showed full rescue (2.63%), 9 strong rescue (11.84%), 10 weak rescue (13.16%) and 55 no rescue (72.37%), respectively. To determine whether the different degrees of phenotype rescue was related to the amount of *TrPI* expression in *pi-1* mutants, quantitative real-time RT-PCR analysis was performed from the inflorescences of the different degrees rescued lines. The results indicated that there was a strong positive correlation between transgene expression and degree of rescue. In strong rescued plants, the 35S:: *TrPI* transgene in *pi-1* was expressed at approximately 8-10 times the level of the weak and no rescue plants (Fig. S2). In addition, regardless of rescue degrees, all rescued plants showed carpels that were fused well (Fig. 6B-F), as in the wild-type.

3.4. Interaction patterns of the TrPI protein

In this study, we explored the protein interaction pattern of the TrPI protein by using yeast two-hybrid assays. Transformed yeast cells expressing the protein TrPI together with TrPI, TrAP1, TrFUL or TrSEP3, respectively, grow very robustly in medium lacking Leu, Trp, Ade and His, and can activate the expression of the LacZ reporter gene. In addition, yeast cells co-transformed with the fusion proteins of TrPI and TrTM6 can grow weakly on the selective media lacking Leu, Trp, Ade and His, whereas the expression of the LacZ reporter gene is not activated. None of the reporter genes are activated when TrPI combined with TrAG, or TrSHP are co-transformed into yeast cells. The consensus results were obtained by swapping the DNA-BD and AD fusion vectors. The results show that TrPI formed homodimers, and interacted with TrAP1, TrFUL and TrSEP3, but not with TrAG or TrSHP (Fig. 7). The other MADS-

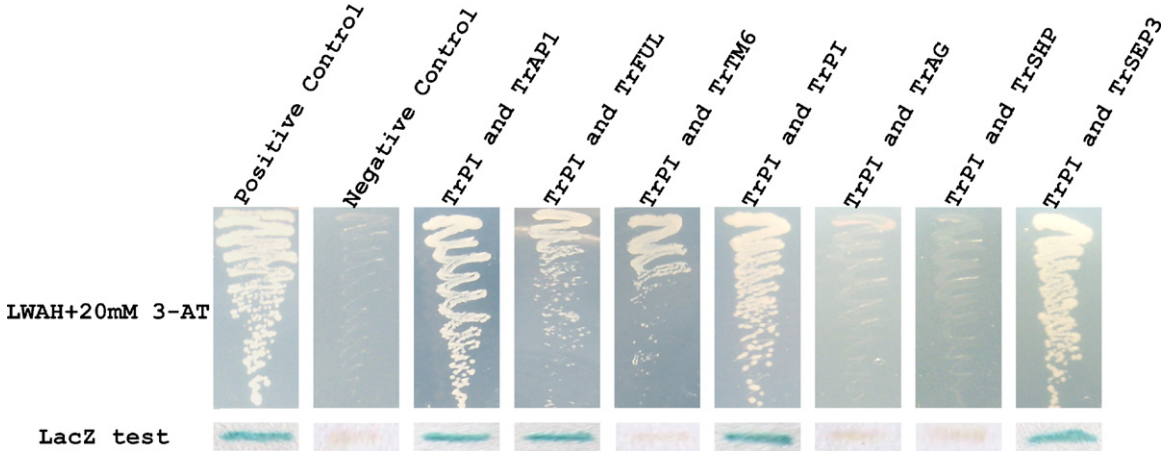

Fig. 7. Interaction analyses of TrPI respectively with other MADS-box proteins isolated from *T. rupestris*. LWAH + 20 mM 3-AT, selective dropout medium lacking leucine, tryptophan, histidine and adenine supplemented with 20 mM 3-aminotriazole; LacZ test, β-galactosidase reporter gene assay.

domains proteins of *T. rupestris* were described previously and have no self-activation by detecting growth on selective dropout medium lacking Leu, Trp, His and Ade supplemented with 20 mM 3-aminotriazole and β-galactosidase reporter gene assay (Lü et al., 2007).

4. Discussion

In this study, a *PI*/*GLO*-like B class MADS-box gene, *TrPI* from *T. rupestris* (Rosaceae), was characterized by both expression studies and functional analyses in transgenic plants. RT-PCR and *in situ* hybridization analyses revealed that *TrPI* is expressed in petal and stamen primordia, and that its expression is maintained until petals and stamens have fully developed. The expression patterns of *TrPI* in floral whorls 2 and 3 are therefore similar to that of *PI*, *GLO* and *PhGLO1/2*. All of these genes are expressed in the regions that will develop into petals and the stamens, the petal and stamen primordia, and their expression in these organs persists through later stages of differentiation (Angenent et al., 1992; Jack et al., 1992; Schwarz-Sommer et al., 1992; van der Krol et al., 1993; Vandenbussche et al., 2004). Our results suggest that *TrPI* in *T. rupestris* functions in specifying the identities of petals and stamens. *TrPI* under the control of a 2 × 35S promoter was sufficient to rescue a null *Arabidopsis pi* mutant, providing evidence that the function of *PI*/*GLO*-like homologs, in line with their expression, for the male reproductive organs and the petals is likely to be highly conserved within the eudicots (Zahn et al., 2005).

In some angiosperm species, transcripts of *PI*/*GLO*-like MADS-box genes are detected in nonfloral organs. For example, *AmtrPI* in *Amborella* and *EGM2* in *Eucalyptus* are expressed in leaves (Southerton et al., 1998; Kim et al., 2005). *ZMM16* in maize is expressed in the leaves, roots, and young seedlings (Münster et al., 2001). *EhPI* in winter aconite *Eranthis* is expressed in the leaves, stems and honey leaves (Skipper, 2002). However, the exact functions, if any, of these vegetative expression domains have not yet been defined. In this study, in addition to expression in petals and stamens, *TrPI* transcripts are also detected in both young leaves and inflorescence stems. Ectopic expression of *TrPI* in *Arabidopsis* causes remarkable modifications of plant architecture, including non-spiral rosette leaves and cauline leaves, and oblate primary inflorescence stem that produced offshoots. The phenotypes of *35S*::*TrPI* transgenic plants are distinct from those of *35S*::*PI* expressed in *Arabidopsis*. The transgenic *Arabidopsis* plants containing *35S*::*PI* only showed sepals that are transformed into petal-like organs (Krizek and Meyerowitz, 1996; Yang et al., 2003). However, when both *PI* and *AP3* are simultaneously ectopically expressed in *Arabidopsis*, in addition to the floral organs in whorls 1 and 2 developing as petals, and as stamens in whorls 3 and 4, the rosette and cauline leaves are curved upwards and become smaller, and cauline leaves in apical-most positions are often petal-like (Yang et al., 2003).

It has been shown that MADS-domain proteins form specific homodimers or heterodimers to function (Winter et al., 2002; Immink et al., 2003; de Folter et al., 2005; Leseberg et al., 2008). In this study, we analyzed the interaction map of *TrPI* using yeast two-hybrid assays. Although several characteristic positions, e.g. Glu-97, Asn-98, Gly-110, and Gly-131, which might facilitate formation of heterodimers between a PI-like protein and an euAP3-like protein (Yang et al., 2003) were conserved, TrPI is able to form homodimers. This interaction is remarkably different from those of its counterparts in *Arabidopsis*, *Antirrhinum*, and *Petunia*. In these model species, heterodimers, but not homodimers, must form between class B AP3-like and PI-like MADS-domain proteins (Davies et al., 1996; Riechmann et al., 1996). However, outside of the model plants, several PI/GLO-like homodimers have been identified, such as GGM2 in gymnosperm, TGGLO in tulip and LRGLOA or LRGLOB in lily (Winter et al., 2002; Kanno et al., 2003). In this study, heterodimers formed between TrPI with TrAP1, TrFUL and TrSEP3, respectively. In contrast, direct interactions were not found between proteins representing the B-function and A- or C-function proteins in *Arabidopsis*, *Antirrhinum* and *Petunia*. A-function proteins can interact with B-function proteins by bridging of heterodimers formed between one PI/GLO-like and one AP3/DEF-like MADS-box domain protein (Davies et al., 1996; Egea-Cortines et al., 1999; Yang et al., 2003; Kaufmann et al., 2005). The I and K domains of PI are important for both the strength and specificity of AP3/PI heterodimer formation (Yang et al., 2003). The low similarity in the I and K domains between TrPI and PI (Figure 1A; Table S2) might contribute to the formation of different interaction profiles. These data show that, at least in yeast, TrPI has unique protein interaction properties that may contribute to distinct developmental roles. Taken together, these results indicate that the TrPI protein has biochemical features that distinguish it from its well-studied orthologs, PI and GLO. Hence, we hypothesize that *TrPI* might function in regulating vegetative architecture in addition to its putative function as a floral organ identity gene in *T. rupestris*.

Acknowledgments

We thank Jiwei Wang, Miaomiao Zhang, Na Li and Juanjuan Liu for lab assistance. We also thank Drs. Shaobo Jia and Yong Huang for using the anatomical lens. We are grateful to Prof. Dr. Günter Theissen for critical reading of the manuscript. This work was supported by National Nature Science Foundation of China (Grants 30800066, 30770212).

Appendix A. Supplementary data

Supplementary data associated with this article can be found, in the online version, at doi:10.1016/j.jplph.2010.06.028.

References

Alvarez-Buylla ER, Liljegren SJ, Pelaz S, Gold SJ, Burgeff C, Ditta GS, Vergara-Silva F, Yanofsky MF. MADS-box gene evolution beyond flowers: expression in pollen, endosperm, guard cell, and trichomes. Plant J 2000;24:1–11.

Angenent GC, Busscher M, Franken J, Mol JN, van Tunen AJ. Differential expression of two MADS box genes in wild-type and mutant petunia flowers. Plant Cell 1992;4:983–93.

Angenent GC, Franken J, Busscher M, Colombo L, van Tunen AJ. Petal and stamen formation in petunia is regulated by the homeotic gene *fbp1*. Plant J 1993;3:101–12.

APGII. (The Angiosperm Phylogeny Group) An update of the Angiosperm Phylogeny Group classification for the orders and families of flowering plants: APG II. Bot J Linn Soc 2003; 141: 399-436.

Becker A, Theissen G. The major clades of MADS-box genes and their role in the development and evolution of flowering plants. Mol Phylogenet Evol 2003;29:464–89.

Causier B, Kieffer M, Davies B. MADS-Box Genes Reach Maturity. Science 2002;296:275–6.

Clough SJ, Bent AF. Floral dip: a simplified method for *Agrobacterium*-mediated transformation of *Arabidopsis thaliana*. Plant J 1998;16:735–43.

Coen ES, Meyerowitz EM. The war of the whorls: Genetic interactions controlling flower development. Nature 1991;353:31–7.

Davies B, Egea-Cortines M, de Andrade Silva E, Saedler H, Sommer H. Multiple interaction amongst floral homeotic proteins. EMBO J 1996;15:4330–43.

de Folter S, Immink RGH, Kieffer M, Parˇenicovaˇ L, Henz SR, Weigel D, Busscher M, Kooiker M, Colombo L, Kater MM, Davies B, Angenent GC. Comprehensive interaction map of the Arabidopsis MADS box transcription factors. Plant Cell 2005;17:1424–33.

Du XQ, Xiao QY, Zhao R, Wu F, Xu QJ, Chong K, Meng Z. *TrMADS3*, a new MADS-box gene, from a perennial species *Taihangia rupestris* (Rosaceae) is up-regulated by cold and experiences seasonal fluctuation in expression level. Dev Genes Evol 2008;218:281–92.

Egea-Cortines M, Saedler H, Sommer H. Ternary complex formation between the MADS-box proteins SQUAMOSA, DEFICIENS and GLOBOSA is involved in the control of floral architecture in *Antirrhinum majus*. EMBO J 1999;18:5370–9.

Goto K, Meyerowitz EM. Function and regulation of the *Arabidopsis* floral homeotic gene *PISTILLATA*. Genes Dev 1994;8:1548–60.

Immink RGH, Ferrario S, Busscher-Lange J, Kooiker M, Busscher M, Angenent GC. Analysis of the petunia MADS-box transcription factor family. Mol Genet Genomics 2003;268:598–606.

Irish VF, Litt A. Flower development and evolution: gene duplication, diversification and redeployment. Curr Opin Genet Dev 2005;15:454–60.

Jack T, Brockman LL, Meyerowitz EM. The homeotic gene *APETALA3* of *Arabidopsis thaliana* encodes a MADS box and is expressed in petals and stamens. Cell 1992;68:683–97.

Jack T, Fox GL, Meyerowitz EM. Arabidopsis homeotic gene *APETALA3* ectopic expression: Transcriptional and posttranscriptional regulation determine floral organ identity. Cell 1994;76:703–16.

Kanno A, Saeki H, Kameya T, Saedler H, Theissen G. Heterotopic expression of class B floral homeotic genes supports a modified ABC model for tulip (*Tulipa gesneriana*). Plant Mol Biol 2003;52:831–41.

Kaufmann K, Melzer R, Theissen G. MIKC-type MADS-domain proteins: structural modularity, protein interactions and network evolution in land plants. Gene 2005;347:183–98.

Kim S, Koh J, Yoo MJ, Kong HZ, Hu Y, Ma H, Soltis PS, Soltis DE. Expression of floral MADS-box genes in basal angiosperms: implications for the evolution of floral regulators. Plant J 2005;43:724–44.

Kitahara K, Hirai S, Fukui H, Matsumoto S. Rose MADS-box genes 'MASAKO BP and B3' homologous to class B floral identity genes. Plant Sci 2001;161:549–57.

Kitahara K, Ohtsubo T, Soejima J, Matsumoto S. Cloning and characterization of apple class B MADS-box genes including a novel AP3 homologue MdTM6. Engei Gakkai Zasshi 2004;73:208–15.

Kramer EM, Dorit RL, Irish VF. Molecular evolution of genes controlling petal and stamen development: duplication and divergence within the *APETALA3* and *PISTILLATA* MADS-box gene lineages. Genetics 1998;149:765–83.

Krizek BA, Meyerowitz EM. The Arabidopsis homeotic genes *APETALA3* and *PISTILLATA* are sufficient to provide the B class organ identity function. Development 1996;122:11–22.

Lü SH, Du XQ, Lu WL, Chong K, Meng Z. Two *AGAMOUS*-like MADS-box genes from *Taihangia rupestris* (Rosaceae) reveal independent trajectories in the evolution of class C and class D floral homeotic functions. Evol Dev 2007;9:92–104.

Lamb RS, Irish VF. Functional divergence within the *APETALA3*/*PISTILLATA* floral homeotic gene lineages. Proc Natl Acad Sci USA 2003;100:6558–63.

Leseberg CH, Eissler CL, Wang X, Johns MA, Duvall MR, Mao L. Interaction study of MADS-domain proteins in tomato. J Exp Bot 2008;59:2253–65.

Li GS, Meng Z, Kong HZ, Chen ZD, Theissen G, Lu AM. Characterization of candidate class A, B and E floral homeotic genes from the perianthless basal angiosperm *Chloranthus spicatus* (Chloranthaceae). Dev Genes Evol 2005;215:1–13.

Münster T, Wingen LU, Faigl W, Werth S, Saedler H, Theissen G. Characterization of three *GLOBOSA*-like MADS-box genes from maize: evidence for ancient paralogy in one class of floral homeotic B-function genes of grasses. Gene 2001;262:1–13.

Ma H, Yanofsky MF, Meyerowitz EM. AGL1-AGL6, an Arabidopsis gene family with similarity to floral homeotic and transcription factor genes. Genes Dev 1991;5:484–95.

Riechmann JL, Krizek BA, Meyerowitz EM. Dimerization specificity of Arabidopsis MADS domain homeotic proteins APETALA1, APETALA3, PISTILLATA, and AGAMOUS. Proc Natl Acad Sci USA 1996;93:4793–8.

Schwarz-Sommer Z, Hue I, Huijser P, Flor PJ, Hansen R, Tetens F, Lonnig WE, Saedler H, Sommer H. Characterization of the *Antirrhinum* floral homeotic MADS-box gene deficiens: evidence for DNA binding and autoregulation of its persistent expression throughout flower development. EMBO J 1992;11:251–63.

Skipper M. Genes from the *APETALA3* and *PISTILLATA* lineages are expressed in developing vascular bundles of the tuberous rhizome, flowering stem and flower primordia of *Eranthis hyemalis*. Ann Bot (LOND) 2002;89:83–8.

Soltis PS, Soltis DE, Chase MW. Angiosperm phylogeny inferred from multiple genes as a tool for comparative biology. Nature 1999;402:402–4.

Sommer H, Beltran JP, Huijser P, Pape H, Lonnig WE, Saedler H, Schwarz-Sommer Z. Deficiens, a homeotic gene involved in the control of flower morphogenesis in *Antirrhinum majus*: the protein shows homology to transcription factors. EMBO J 1990;9:605–13.

Southerton SG, Marshall H, Mouradov A, Teasdale RD. Eucalypt MADS-box genes expressed in developing flowers. Plant Physiol 1998;118:365–72.

Su KM, Zhao SZ, Shan HY, Kong HZ, Lu WL, Theissen G, Chen ZD, Meng Z. The MIK region rather than the C-terminal domain of AP3-like class B floral homeotic proteins determines functional specificity in the development and evolution of petals. New Phytol 2008;178:544–58.

Tani E, Polidoros AN, Flemetakis E, Stedel C, Kalloniati C, Demetriou K, Katinakis P, Tsaftaris AS. Characterization and expression analysis of *AGAMOUS*-like, *SEEDSTICK*-like, and *SEPALLATA*-like MADS-box genes in peach (*Prunus persica*) fruit. Plant Physiol Biochem 2009;47:690–700.

Theissen G, Becker A, Di Rosa A, Kanno A, Kim JT, Munster T, Winter KU, Saedler H. A short history of MADS-box genes in plants. Plant Mol Biol 2000;42:115–49.

Trobner W, Ramirez L, Motte P, Hue I, Huijser P, Lonnig WE, Saedler H, Sommer H, Schwarz-Sommer Z. GLOBOSA: a homeotic gene which interacts with DEFICIENS in the control of *Antirrhinum* floral organogenesis. EMBO J 1992;13:4693–704.

Tsuchimoto S, Mayama T, van der Krol A, Ohtsubo E. The whorl-specific action of a petunia class B floral homeotic gene. Genes Cells 2000;5:89–99.

van der Krol AR, Brunelle A, Tsuchimoto S, Chua NH. Functional analysis of petunia floral homeotic MADS box gene *pMADS1*. Genes Dev 1993;7:1214–28.

van der Linden CG, Vosman B, Smulders MJM. Cloning and characterization of four apple MADS box genes isolated from vegetative tissue. J Exp Bot 2002;53:1025–36.

Vandenbussche M, Zethof J, Royaert S, Weterings K, Gerats T. The duplicated B-class heterodimer model: whorl-specific effects and complex genetic interactions in *Petunia hybrida* flower development. Plant Cell 2004;16:741–54.

Winter KU, Weiser C, Kaufmann K, Bohne A, Kirchner C, Kanno A, Saedler H, Theissen G. Evolution of class B floral homeotic proteins: obligate heterodimerization originated from homodimerization. Mol Biol Evol 2002;19:587–96.

Xu YY, Wang XM, Li J, Li JH, Wu JS, Walker JC, Xu ZH, Chong K. Activation of the *WUS* gene induces ectopic initiation of floral meristems on mature stem surface in *Arabidopsis thaliana*. Plant Mol Biol 2005;57:773–84.

Yang Y, Fanning L, Jack T. The K domain mediates heterodimerization of the Arabidopsis floral organ identity proteins, APETALA3 and PISTILLATA. Plant J 2003;33:47–59.

Yao J, Dong Y, Morris BA. Parthenocarpic apple fruit production conferred by transposon insertion mutations in a MADS-box transcription factor. Proc Natl Acad Sci USA 2001;98:1306–11.

Yao JL, Dong YH, Kvarnheden A, Morris B. Seven MADS-box genes in apple are expressed in different parts of the fruit. J Am Soc Hortic Sci 1999;124:8–13.

Zahn LM, Leebens-Mack J, dePamphilis CW, Ma H, Theissen G. To B or not to B a flower: the role of DEFICIENS and GLOBOSA orthologs in the evolution of the angiosperms. J Heredity 2005;96:225–40.

Zhang L, Xu Y, Ma R. Molecular cloning, identification, and chromosomal localization of two MADS box genes in peach (*Prunus persica*). J Genet Genomics 2008;35:365–72.